Tonkie Khimicheskie Tekhnologii = Fine Chemical Technologies.
2025;20(5):454–473 ISSN 2686-7575 (Online)

UDC 661.727.83
https://doi.org/10.32362/2410-6593-2025-20-5-454-473
EDN NYBHED

RESEARCH ARTICLE

Dichloromethane solvent for furfural recovery from potato peels: Thermodynamic and kinetic investigations

Abdulhalim Musa Abubakar[1,✉], Iyisikwe Tanimu Umar[1], Abass-Giwa Muhammed Akintunde[2], Muhammad Jimada Aliyu[3], Marwea Al-Hedrewy[4,5], Uday Raheja[6]

[1] *Department of Chemical Engineering, Faculty of Engineering, Modibbo Adama University, P.M.B. 2076, Yola, Adamawa State, Nigeria*

[2] *Department of Chemical Engineering, Faculty of Engineering, University of Maiduguri, P.M.B. 1069, Bama Road, Maiduguri, Borno State, Nigeria*

[3] *Chemical Engineering Department, School of Infrastructure, Process Engineering and Technology, Federal University of Technology, Minna, Niger State, Nigeria*

[4] *College of Technical Engineering, the Islamic University, Najaf, Iraq*

[5] *College of Technical Engineering, the Islamic University of Al Diwaniyah, Al Diwaniyah, Iraq*

[6] *Center for Research Impact & Outcome, Chitkara University Institute of Engineering and Technology (CUIET), Chitkara University, Rajpura, 140401, Punjab, India*

✉ *Corresponding author, e-mail: abdulhalim@mau.edu.ng*

Abstract

Objectives. This study aims to investigate the kinetics and thermodynamics of furfural extraction from sweet potato peels using dichloromethane (CH_2Cl_2) as a solvent and sulfuric acid as a catalyst. To that end, we set out to determine the kinetic parameters for furfural production using first- and second-order models, optimize the extraction temperature, and evaluate the thermodynamic properties of the reaction.

Methods. Potato peels, selected for their high hemicellulose content, cost-effectiveness, and sustainability, were processed with dichloromethane, selected for its safety, low energy requirements, and compatibility with green extraction processes. Experimental conditions involved varying temperatures (60, 70, and 80°C) and peel powder particle sizes (<5 mm), with the reaction being monitored to fit kinetic models and calculate thermodynamic properties.

Results. Experimental findings revealed that the first-order kinetic model provided the best fit, with an activation energy (E_a) of 85.99 kJ/mol. Thermodynamic analysis showed an enthalpy change (ΔH) of 83.14 kJ/mol, entropy change (ΔS) of −86.08 J/(mol·K), and Gibbs free energy (ΔG) values ranging from 111.80 to 112.66 kJ/mol across the studied temperatures. Optimal extraction conditions were achieved at 80°C, yielding the highest furfural concentration through acid-catalyzed hydrolysis. The energy-intensive yet controlled nature of the reaction highlights the need for further optimization.

Conclusions. This study demonstrates the effectiveness of dichloromethane as a solvent for furfural extraction from sweet potato peels under optimized conditions. The kinetic and thermodynamic findings elucidate the reaction mechanism and its industrial applicability. Future studies should focus on simulating furfural separation from ternary solvent systems using Aspen Plus to enhance sustainability and scalability.

Keywords
furfural extraction, dichloromethane, potato peels, extraction kinetics, Eyring–Polanyi model

Submitted: 13.01.2025
Revised: 17.03.2025
Accepted: 03.09.2025

For citation
Abubakar A.M., Umar I.T., Akintunde A.-G.M., Aliyu M.J., Al-Hedrewy M., Raheja U. Dichloromethane solvent for furfural recovery from potato peels: Thermodynamic and kinetic investigations. *Tonk. Khim. Tekhnol. = Fine Chem. Technol.* 2025;20(5):454–473. https://doi.org/10.32362/2410-6593-2025-20-5-454-473

НАУЧНАЯ СТАТЬЯ

Экстракция фурфурола из картофельной шелухи с помощью дихлорметана: термодинамика и кинетика

Abdulhalim Musa Abubakar[1]✉, Iyisikwe Tanimu Umar[1], Abass-Giwa Muhammed Akintunde[2], Muhammad Jimada Aliyu[3], Marwea Al-Hedrewy[4,5], Uday Raheja[6]

[1] *Department of Chemical Engineering, Faculty of Engineering, Modibbo Adama University, P.M.B. 2076, Yola, Adamawa State, Nigeria*

[2] *Department of Chemical Engineering, Faculty of Engineering, University of Maiduguri, P.M.B. 1069, Bama Road, Maiduguri, Borno State, Nigeria*

[3] *Chemical Engineering Department, School of Infrastructure, Process Engineering and Technology, Federal University of Technology, Minna, Niger State, Nigeria*

[4] *College of Technical Engineering, the Islamic University, Najaf, Iraq*

[5] *College of Technical Engineering, the Islamic University of Al Diwaniyah, Al Diwaniyah, Iraq*

[6] *Center for Research Impact & Outcome, Chitkara University Institute of Engineering and Technology (CUIET), Chitkara University, Rajpura, 140401, Punjab, India*

✉ *Автор для переписки, e-mail: abdulhalim@mau.edu.ng*

Аннотация

Цели. Целью данного исследования является изучение кинетики и термодинамики экстракции фурфурола из кожуры сладкого картофеля с использованием дихлорметана (CH_2Cl_2) в качестве растворителя и серной кислоты в качестве катализатора. Для этого было решено определить кинетические параметры производства фурфурола, используя модели первого и второго порядка, оптимизировать температуру экстракции и оценить термодинамические свойства реакции.

Методы. Картофельная кожура была выбрана для экстракции фурфурола из-за высокого содержания в ней гемицеллюлозы, экономичности и экологичности. В качестве растворителя был выбран дихлорметан благодаря его безопасности, низкой энергоемкости и совместимости с экологически чистыми процессами экстракции. Условия эксперимента включали варьирование температур (60, 70 и 80°C) и размеров частиц порошка (<5 мм). В процессе эксперимента осуществлялся контроль на соответствие реакции кинетическим моделям и расчет термодинамических характеристик.

Результаты. Экспериментальные результаты показали, что кинетическая модель первого порядка лучше описывает реакцию, энергия активации (E_a) равна 85.99 кДж/моль. Термодинамический анализ показал изменение энтальпии (ΔH) на 83.14 кДж/моль, изменение энтропии (ΔS) на −86.08 Дж/(моль·К), а свободная энергия Гиббса (ΔG) варьировалась от 111.80 до 112.66 кДж/моль в зависимости от выбранных температур. При температуре 80°C были достигнуты оптимальные условия экстракции, и получена наиболее высокая концентрацию фурфурола методом гидролиза с использованием серной кислоты в качестве катализатора. Реакция имеет энергоемкий, но контролируемый характер, что говорит о необходимости дальнейшей оптимизации процесса.

Выводы. Исследование продемонстрировало эффективность дихлорметана в качестве растворителя для экстракции фурфурола из кожуры сладкого картофеля при оптимальных условиях. Кинетические и термодинамические результаты проясняют механизм реакции и обосновывают ее промышленное применение. Будущие исследования должны быть сосредоточены на моделировании выделения фурфурола из тройных систем растворителей с использованием Aspen Plus для повышения устойчивости и масштабируемости.

Ключевые слова
экстракция фурфурола, дихлорметан, картофельная шелуха, кинетика экстракции, модель Эйринга–Полани

Поступила: 13.01.2025
Доработана: 17.03.2025
Принята в печать: 03.09.2025

Для цитирования
Abubakar A.M., Umar I.T., Akintunde A.-G.M., Aliyu M.J., Al-Hedrewy M., Raheja U. Dichloromethane solvent for furfural recovery from potato peels: Thermodynamic and kinetic investigations. *Tonk. Khim. Tekhnol. = Fine Chem. Technol*. 2025;20(5):454–473. https://doi.org/10.32362/2410-6593-2025-20-5-454-473

INTRODUCTION

Furfural (or furan-2-carbaldehyde, $C_5H_4O_2$) is a colorless or yellowish aromatic aldehyde with a furan ring (a 5-membered aromatic ring containing 1 oxygen atom) and an aldehyde group (–CHO) attached to the 2-position of the furan ring [1, 2]. It finds application in diverse areas, including oil and gas (such as, jet fuel blend stocks), petroleum refining (as a solvent), medicine (e.g., for creation of tuberculosis remedies, as well as antimicrobial, antibiotic, or antifungal agents), agriculture (as a fertilizer, insecticide, nematicide, fungicide or herbicide), food science technology (e.g., flavoring agent), pharmaceuticals, plastic (synthetic fibers and phenolic resins), milling (grinding and abrasive wheels), detergents, cosmetics, rubber, nylon, polymer (as a polyurethane-polyurea copolymer), construction, metal coatings, biofuel and chemical production (pyrrole, pyrrolidine, lysine, lubricants, adhesives, dihydropyran, furan, furfuryl alcohol, tetrahydrofuran, furoic acid, and methyltetrahydrofuran) [3–7]. The precursors of furfural are the arabinan, xylan, and pentosan components derived from agricultural waste rich in hemicellulose and other lignocellulosic materials [8, 9], such as sawdust, rice straw, cotton seed hull bran, flax shives, hazelnut shells, spruce wood, beech wood, pine wood, Douglas-fir wood, poplar, corn stover, oat hulls, sunflower hull, cotton husk, almond shells, corncob, barley hull, sorghum straw, and sugarcane bagasse [10–12]. In [13], Clauser *et al*. used the technology of steam explosion pretreatment of pine sawdust and evaluated the economic, mass, and energy balances involved in furfural recovery from a jacketed batch reactor. Ideally, hemicellulose hydrolysis releases pentoses (e.g., xylose), which are capable of dehydrating under acidic conditions to form furfural [14, 15]. The examples include the stripping of furfural from pentosan-rich corncob by Agirrezabal–Telleria *et al*. [16] and rice husk by Nunez *et al.* [17]. The list of catalysts includes superheated water [18], ionic liquids [19, 20], metallic oxides [11], chlorides (e.g., $AlCl_3$, $FeCl_3$, NaCl, $CaCl_2$, $MgCl_2$, $SnCl_4$, and $CuCl_2$) [21, 22], enzyme [23], silicoaluminophosphate (e.g., SAPO-44) [24], *p*-TsOH [25], γ-alumina (γ-Al_2O_3) [15], HZSM-5 zeolite [26], H-β-zeolite [27], betaine [28], formic acid [29], acetic acid [30], maleic acid [31], hydrochloric acid [32], sulfuric acid [33, 34], phosphoric acid [35], hectorites, fluorohectorites [36], Lewis and Brønsted acid [37, 38]. These are employed via hydrothermal [39] or other processes, as shown in Table 1. Ji *et al.* [25] and Weidener *et al.* [35] proposed a novel recycling scheme as a sustainable and economically feasible way of utilizing mineral acid catalyst to reduce costs and environmental intoxication, as possible solutions to the challenges highlighted in Zhang *et al.* [40], Yong *et al.* [41], and Muryanto *et al.* [42]. The scheme of the aforementioned authors can be extended to extraction projects employing acid solvents as reported by Lee and Wu [43] (see Table 1), despite the need to exercise caution when applying deep eutectic solvents (DES) as mentioned in [44].

Table 1. Biomass employed previously for the extraction of furfural

Method	Solvent	Raw material	Reaction/Extraction parameters	Author
Thermochemical process (supercritical conditions)	Supercritical ethanol	Oil palm	Temp. = 240–280°C; reaction time = 1–30 min; biomass solid loading = 0.4–0.8 g; alcohol/acid ratios = 1 : 1 and 1 : 2	[7]
Subcritical thermochemical process	Subcritical ethanol	Oil palm frond	Temp. = 230°C; reaction time = 20 min; solid loading = 1 g	[45]
Hydrolysate dehydration	Sulfuric acid	Dried oil palm empty fruit bunch	Temp. = 198°C and reaction time = 11 min	[46]

Table 1. Continued

Method	Solvent	Raw material	Reaction/Extraction parameters	Author
Liquid–liquid extraction	Methyl isobutyl ketone (MIBK)	Oil palm empty fruit bunch	Temp. = 105°C and reaction time = 30 min	[47]
Acid hydrolysis followed by dehydration	Sulfuric acid	Oil palm empty fruit bunch	Reaction time = 90 min and 15% acid	[48]
Steam explosion	Sulfuric acid	Oil palm trunk	Temp. = 110, 130, and 170°C; reaction time = 2 and 3 h	[49]
Non-isothermal autohydrolysis	–	Wheat straw and *Eucalyptus globulus*	Temp. = 220°C	[6]
Microwave-assisted process	Hydrochloric acid	Wheat straw	pH 0.22 or 1.77; temp. = 146 or 195°C; L : S ratios = 84 or 90 mL/g; residence times = 31 or 34 min	[32]
Microwave irradiations	MIBK	Wheat straw	Reaction time = 1–2 h and temp. = 120–150°C	[28]
Isothermal autohydrolysis	–	Eucalyptus globulus	Temp. = 220°C and reaction time = 60 min	[50]
Acid hydrolysis	–	Eucalyptus globulus	Medium operation time = 15 min; low temperature = 170°C; pH 2	[51]
Microwave-assisted process	Sulfuric acid	Olive stone	Temp. = 200°C and the addition of 0.1 M $FeCl_3$	[52]
Dilute-acid hydrolysis	Sulfuric acid	Olive stone	Temp. < 40°C and reaction time < 120 s	[34]
Distillation and transesterification reaction	Butanol	Algae and switchgrass	Temp. = 30°C, pressure = 4 bar, time = 8 h, and water amount = 0 g	[23]
Non-isothermal autohydrolysis	MIBK	Birch (*Betula alba*) wood	Temp. = 170°C and reaction time = 60 min	[53]
Acid hydrolysis	Sulfuric acid	Birch wood	Biomass pretreatment time = 90 min	[9]
Acid hydrolysis	Sulfuric acid	Birch wood	Temp. = 147°C and reaction time = 90 min	[54], [55]
In vitro spectrophotometric assays	Fungi metabolism	Cellulose garbage	pH 5.5 and incubation time = 14 days	[5]
Autohydrolysis and separation	Chloroform	Southern cattail (*Typha domingensis*)	Temp. = 177–189°C and reaction time = 30–45 min	[56]
Acid hydrolysis	Sulfuric acid	Pistachio green hulls	Reaction temp. = 152–272°C; acid concentration = 0.5–4.0 mol/L; reaction time = 30–600 s	[57]
Enzymatic hydrolysis	MIBK–water biphasic system	Corn bran	10% KOH solution and aqueous ethanol solution = 40–90%	[58]
N_2- and steam-stripping	Toluene	Corncob	Experimental and Aspen Plus simulation data	[16]
Steam distillation	–	Corncob	Temp. = 180°C and reaction time = 30 min	[21]
Steam distillation at hydrolysis conditions	Concentrated seawater	Corncob	Temp. = 190°C	[59]
Hydrodistillation and autohydrolysis Kraft process	Sulfuric, hydrochloric, and phosphoric acids	Corncobs, sugarcane bagasse, and eucalypt wood	Acid concentration = 1.5–5.2 mol/L	[60]
Acid hydrolysis	Sulfuric acid	Sugarcane bagasse, *Eucalyptus globulus*, and *Acacia longifolia*	Temp. = 150–170°C and reaction time = 30–90 min	[61]

Table 1. Continued

Method	Solvent	Raw material	Reaction/Extraction parameters	Author
Acid hydrolysis	Sulfuric acid	Rice husk	Temp. = 200°C; acid concentration = 0.1% (*w*/*w*); reaction time = 40 min	[62]
Distillation and separation	Sulfuric acid	Rice straw and bagasse	Evaporator temp. = 40°C and acid volume = 4.17 L	[63]
Distillation process	Chloroform	Rice straw	Evaporator temp. = 4°C	[64]
Acid hydrolysis	Sulfuric acid	Rice husk and bagasse	S : L ratio = 1 : 15; temp. = 180°C; 0.4% acid	[65]
Distillation process	Water	Bagasse	Temp. = 170–200°C and reaction time = 40 min	[10]
Distillation process	Hexane	Sugarcane bagasse	S : L ratio = 1 : 15 and temp. = 110°C	[66]
Distillation process	Dichloromethane	Sugarcane bagasse	S : L ratio = 1 : 15; temp. = 110°C; steam pressure = 1.05 kg/cm^2	[67]
Hydrolysis	Phosphoric acid	Sugarcane bagasse	Acetone/water ratio = 7 : 3 *v*/*v* and temp. = 150°C	[68]
Acid hydrolysis	Glycine-based ionic liquid	Sugarcane bagasse	Temp. = 180°C; reaction time = 10 min; 10 eq. of ionic liquid	[69]
One-pot processing	Toluene–water	Bagasse, rice husk, and wheat straw	Temp. = 170°C and reaction time = 10 h	[24]
One-pot system and BRD	*p*-TsOH	Corncob	Effect of temperature and time	[70]
Acid hydrolysis	Sulfuric acid	Corncob	Temp. = 60–160°C; reaction time = 30–90 min; acid concentration = 5–20 wt %	[25]
Acid hydrolysis	Sulfuric acid	Corncob	Temp. = 140–200°C and pressure = 350–1550 kPa	[18]
Microwave irradiation	γ-Valerolactone	Corncob	Temp. = 190°C and S : L ratio = 1 : 20	[71]
Hydrolysis	Sulfuric acid–toluene biphasic system	Corncob	Water/solid ratio ≤ 1 and reaction time = 10 min	[72]
Enzymatic hydrolysis	Ethanol	Milled wood lignin and corncob	Involves Soxhlet extraction	[73]
Microwave-assisted	Butyl acetate–NaCl biphasic system	Corncob and xylose	Temp. = 160°C and reaction time = 60 min	[74]
Microwave-assisted	Toluene	Almond shells	Reaction time = 1 h	[36]
Steam explosion	–	SELRS	Catalyst = 60 g/kg; reaction temp. = 160°C; extraction steam flow rate = 2.5 cm^3/min; sugar concentration = 61.4 kg/m^3	[26]
Fractionation and enzymatic hydrolysis	Aqueous choline chloride (ChCl)	Switchgrass	Pretreatment temp. = 120°C; extraction temp. = 130–160°C; $AlCl_3$ added = 2% *w*/*v*; reaction time = 15–50 min	[75]
Ultrasonic pretreatment followed by DES reaction	Aqueous ChCl–oxalic acid	Oil palm fronds	Temp. = 120°C and reaction time = 60 min	[76]
Acid-catalyzed hydrolysis	Sulfuric acid	Tea leaves and rice hull	S : L ratio = 25 mL/g and acid concentration = 20% (*w*/*w*)	[11]
Microwave-assisted dehydration	CPME	Xylose, xylan, and rice husk	Temp. = 170°C and pH 1.9–2.3	[29]
Multiphase dehydration	Water	Xylose	Substrate concentration = 1.2 mol L^{-1}; catalyst = 10 mol %; reaction temp. = 120–160°C	[77]

Table 1. Continued

Method	Solvent	Raw material	Reaction/Extraction parameters	Author
Acid hydrolysis	Sulfuric acid	Rice husk and soybean peel	Temp. = 120°C; reaction time = 3 and 4 h	[78]
Acid hydrolysis	Hydrochloric acid, ethanol, and MIPK	Rice straw	Initial xylose concentration = 60 g/L; reaction temp. = 150°C; Pt/Al_2O_3 weight = 0.75 g; acid concentration = 5 wt %	[79]
Acid hydrolysis	Sulfuric acid	Miscanthus	Biomass loading = 9 wt %; acid concentration = 0.5 M; temp. = 185°C	[80]
Soxhlet and distillation	*n*-Hexane	Date palm seed	Humidity = 7.71%; pH 5.5; water activity = 0.365	[81]
Simple distillation	Hexane	Date seed	Distillation temp. = 60°C	[82]
Monophasic system	γ-Valerolactone	Corn fiber, xylose, arabinose, and ribose	10 mL thick-walled glass reactors	[27]
Hydrolysis	Dilute sulfuric acid–MIBK biphasic system	Bamboo	Particle size analysis	[83]
Microwave-assisted	Biphasic medium	Xylose and bamboo	Reaction temp. = 80–160°C; residence time = 0–60 min; water amount = 0–1.2 mL; biphasic medium/substrate ratio = (2 : 1)–(18 : 1)	[84]
LLE and HS-SPME	No need for solvent	Wood hydrolysates	Temp. = 180–200°C and reaction time = 5–15 min	[85]
Hydrolysis	Sulfuric acid	Hardwood	Temp. = 190°C; ZSM-5 = 1 g; NaCl = 1.05 g; solvent-to-aqueous phase ratio = 30 : 15 *v*/*v*; reaction time = 3 h	[86]
Hydrolysis	MIBK	Hardwood PHL	Temp. = 170°C and reaction time = 100 min	[87]
Hydrolysis	Sulfuric acid and acetic acid	Hardwood PHL	Temp. = 150–190°C	[30]
Enzymatic hydrolysis	MTHF	Sugarcane bagasse	0.45 g bagasse; 9 mL MTHF; 9 mL water; 0.1 M $AlCl_3$; temp. = 150°C; reaction time = 45 min; 10 wt % NaCl	[22]
Hydrolysis	Sulfuric acid	Sugarcane bagasse	Temp. = 170°C and acid concentration = 0.25 wt %	[88]
Acid hydrolysis	Sulfuric acid	Orange peel pectin	0.01 M acid; reaction time = 90 min; temp. = 160°C	[89]
Acid hydrolysis	Ethanol	Decorative plants (*Mimusops elengi, Madhuca indica, Hiptage benghalensis*, and *Polyalthia longifolia*)	50 mL ethanol and 50 mL distilled water	[90]
Hydrolysis	Chloroform	Mikania micrantha	50 mL chloroform and distillation temp. = 70°C	[91]
Acid hydrolysis	Hydrochloric acid	Theobrama cacao	Extraction time = 35 min; HCl concentration = 5 M and; amount of NaCl = 7 g	[92]
Microwave and oil bathing heating	MIBK, benzene, cyclohexane, and 1,4-dioxane	*Camellia oleifera* fruit shell	$[Bmim]HSO_4$ catalyst	[93]
Autohydrolysis	Water	Biomass hydrolysate	Temp. = 200°C and reaction time = 3 h	[94]

Table 1. Continued

Method	Solvent	Raw material	Reaction/Extraction parameters	Author
Solvent extraction	Ethyl acetate	Mustard (*Brassica carinata*)	Time = 4–5 h	[95]
Hydrolysis	Butanone–water biphasic system	C5 carbohydrate	Experimental and molecular dynamic simulation	[20]
Hydrolysis	DES	Sunflower stalk	Temp. = 180°C and reaction time = 15 min	[96]
Microwave-assisted	MIBK	Chestnut shell	Temp. = 180°C and reaction time = 15 min	[97]
One-pot processing	ChCl–DES–MIBK biphasic system	Eucalyptus urophylla	Temp. = 140°C and reaction time = 90 min	[98]
Sodium hydroxide hydrogenation	Sulfuric acid	Maize cob, elephant grass, sunflower, and baobab pulp	Temp. = 160°C and reaction time = 160 min	[99]

Note: L : S = liquid–solid; S : L = solid–liquid; MIBK = methyl isobutyl ketone; BRD = batch reaction incorporating distillation; *p*-TsOH = *p*-toluenesulfonic acid; SELRS = steam explosion liquor of rice straw; CPME = cyclopentylmethyl ether; MTHF = 2-methyltetrahydrofuran; MIPK = methyl isopropyl ketone; PHL = pre-hydrolysis liquor; LLE = liquid–liquid extraction; HS-SPME = headspace solid phase microextraction.

According to García *et al.* [56] and Dutta *et al.* [100], from all sources, ≤200–700 kilotons of furfural is produced per annum. The first industrial manufacture occurred between 1921–1923 at Quaker Oats Plant, Iowa, USA [12, 40, 101]. Potato peels as a feedstock for furfural production offer several advantages, including reduced waste generation in the food industry, lower production costs compared to conventional feedstocks, and a potential for higher furfural yields due to the high pentosan content therein. Given its toxicity, efficient extraction of furfural from foods, beverages, or lignocellulosic materials should consider the safety aspect. Exposure to furfural could lead to skin and eye irritation, and trigger liver cancer [64, 102]. It can inhibit growth in plants [103]. The works published during 1991–2024, reviewed as part of this study, revealed zero utilization of potato peels for furfural synthesis. At the same time, Gebre *et al.* [10] mentioned its presence in nectarines and sweet potatoes. Presumably, this gap can be attributed to the complex composition of potato peels and the difficulty of obtaining sufficient/appreciable yield, compared to its conversion to other products such as biobutanol [104] and bioethanol, as well as its application as a adsorbent. The concentration or purity of furfural and its identification is usually carried out using gas chromatography–mass spectrometry (GC–MS), high-performance liquid chromatography (HPLC), nuclear magnetic resonance (NMR) spectroscopy, aniline acetate color reaction, infrared spectrophotometry, ultraviolet–visible spectrophotometry, colorimetric spectrophotometry, and refractive index technologies [56, 81, 105, 106].

Australia and the USA are markets for furfural. The kinetics of furfural production have been studied using plug flow reactors in either single- or two-stage systems and other processes [38, 77, 80], a vapor-releasing reactor system [94], or continuous flow reactors as reported by Nsubuga *et al.* [107], along with its optimization by the Response Surface Methodology (RSM) [47, 61, 69, 88, 92, 108] and Aspen Plus [109], [110]. Thus, Li *et al.* [111] studied the kinetics of furfural yield from corncob using a sulfuric acid catalyst; Xia *et al.* [84] kinetically analyzed the recovery of furfural from xylose and bamboo. Acetic and sulfuric acid catalysts were employed by Liu *et al.* [30] to manufacture furfural PHL hardwood.

To the best of our knowledge, it was only Uppal and Kaur [67] who used dichloromethane (CH_2Cl_2) as a solvent to separate the organic layer in a distillation flask, which Xiang and Runge [112] conflictingly described as an energy-intensive process. Thus, the choice of CH_2Cl_2 as a solvent in our study is governed by the selection criteria discussed by Ye *et al.* [113], in particular, its low energy requirements to balance against its high cost. In addition, we aim to analyze the kinetics and thermodynamics of furfural production when using a sulfuric acid catalyst frequently employed in the literature, to extract furfural from potato peels in view of the significant xylose content therein, earlier pointed out by Gebre *et al.* [10]. The kinetic study includes both first- and second-order furfural production rate analysis, of which only first-order models have thus far been considered. An acid hydrolysis technique is used to determine the energy parameters of the extraction process. Since the physical and chemical properties of potato peels have been comprehensively reported in the literature, we rely on those studies and, instead, concentrate on the gaps identified in Table 1.

Fundamentally, the novelty of this study lies in the use of CH_2Cl_2 solvent and potato peels. According to reports, CH_2Cl_2 is safer than conventional acid types, thereby enabling a greener approach discussed by Cousin *et al.* [114] and lower energy requirements compared to distillation [104].

METHODOLOGY

2.1. Materials and equipment

Furfural extraction from ground potato peels was carried out using CH_2Cl_2 solvent (density = 1.325 g/mL at 20°C; ≥99.9% purity) used by Uppal and Kaur [67], sulfuric acid (5.4% H_2SO_4, approx. 1 M solution) catalyst reported by Iroha *et al.* [115], and water. Further purification of the chemical reagents employed herein was not required [116]. The equipment comprised an R-1001-VN distillation apparatus by *Zhengzhou Wollen Instrument Equipment Co.* (China), a separation funnel by *Shiv Dial Sud & Sons* (India) https://www.shivsons.com/product/separatory-funnel/, a round bottom flask by RB Flask manufacturers, a heating mantle by *Shiv Dial Sud & Sons*, and beakers produced by *HIRSCHMANN* (Germany).

2.2. Potato peel preparation

Fresh sweet potato peels were obtained from the Girei Local Government Area market situated in the Adamawa State, Northeastern Nigeria. It is located based on the GPS coordinate; between latitude 9°22'11.83"N and longitude 12°33'0.74"E, in a close proximity to Yola, the state capital. The collected samples were then washed with tap water before manual size reduction using a steel knife. As shown in Fig. 1, the peel was sun-dried for 4 days before its grinding into powder (size <5 mm) as described by Riera *et al.* [18]. This approach is similar to that used by Mao *et al.* [21], who ensured a particle size of 5–10 mm for the corncob used. It should be noted that no further increase in furfural yield could be achieved when the particle size is reduced to 495 μm, as confirmed by Singh *et al.* [65]. It is typical of 35 mesh sieves[1] in the U.S. Standard Sieve Series (ASTM E11). The use of finely ground potato peel (with a particle size of 500 μm) will significantly reduce internal diffusion resistance by increasing the surface area and enhancing the reactant accessibility.

(a) (b) (c)

Fig. 1. Preparation stages of sweet potato peel: (a) fresh sweet potato peels; (b) dried sweet potato peels; (c) grounded potato peels

Prior to the experiment, personal protective equipment was worn. This included Viton™-made gloves, lab coats, and closed-toe shoes. A ventilated environment was ensured, since the end product (furfural) has a pungent odor smelling like almonds, with a toxicity ranging from highly toxic to relatively non-toxic as based on the records of EPA[2] and Sashikala and Ong [63].

2.3. Extraction of furfural

About 100 g of ground sweet potato peel was weighed and placed into a 500 mL round bottom flask. The hydrolysis process was initiated by adding 200 mL of 1 M H_2SO_4 solution to the flask. Subsequently, the mixture was heated at a temperature of 60°C to reflux for 1 h using a heating mantle [107], adopting a similar duration reported by Sanchez *et al.* [36] who employed a microwave-enhanced process. The mixture (as shown in Fig. 2a) was allowed to cool to room temperature (25°C) then filtered using filter paper to separate the liquid from the solid residues, as mentioned by LaForge [117] and Lee *et al.* [76]. The filtrate (Fig. 2b) was collected in a clean container. The filtrate was transferred into a separatory funnel followed by addition of 50 mL equal volume of nonpolar solvent (in this case, CH_2Cl_2 shown in Fig. 2c) to the separatory funnel. The mixture was then shaken gently for 20 min. Observable layers were allowed to separate naturally, as conducted by Li *et al.* [118]. It should be noted that furfural was expected to be in the organic (lower) layer [87]. The organic layer was later separated and collected in a clean beaker. Next, the organic layer was transferred to a round bottom flask. The procedure was similar to that described by Iriany *et al.* [91] who separated furfural from water using chloroform, resulting in the formation of two layers.

The distillation apparatus was set up as shown in Fig. 2d, and the flask was gently heated to distill off the solvent at 39.6°C. The distillate was collected in a clean

[1] 35 mesh is a medium size of the U.S. Standard mesh size with a 0.0197" (500 μm) nominal sieve opening with a typical wire diameter of 0.315 mm.

[2] EPA, "Pesticide Fact Sheet," 2006, *United States Environmental Protection Agency, Office of Prevention, Pesticide and Toxic Substance* (*7501P*). Available: https://www3.epa.gov/pesticides/chem_search/reg_actions/registration/fs_PC-043301_01-Sep-06.pdf

(a) (b) (c) (d)

Fig. 2. (a) Solution obtained by acid hydrolysis, (b) filtrate after cooling, (c) extraction solvent, and (d) a simple fractional distillation setup

container and heated until the temperature reached 162°C (the boiling point of furfural) in order to isolate the furfural content. The concentration of the oily furfural recovered was then measured at this particular temperature after 1, 1.25, 1.5, and 2 h. It was observed that, when exposed to air, furfural was changing its color from its original colorless/yellowish to a brown-black color, as discussed by Al-Rahbi and Dwivedi [82] and observed by Sashikala and Ong [63] and Gebre *et al.* [10]. At the specified time interval, the experiment was repeated at 70 and 80°C. At least three independent experiments were conducted for each temperature condition to ensure reliability and to minimize experimental error. At the end, only the average values were used to carry out kinetic and thermodynamics analyses.

2.4. Rate law for product formation

In this study, we used no kinetic rate models developed previously [119]. For the first-order rate expression for product formation in Eq. 1, the concentration of furfural is expected to increase over time. Mazar *et al.* [120] emphasized the importance of residence time or reaction time in furfural production.

$$[\mathrm{FF}]_t = [\mathrm{FF}]_{\max}\left(1 - \mathrm{e}^{-kt}\right), \quad (1)$$

wherein $[\mathrm{FF}]_t$ is the concentration of furfural at time t (g/mL), $[\mathrm{FF}]_{\max}$ is the maximum concentration of furfural at equilibrium (g/mL), k is the first-order rate constant, and t is time (h). In order to determine k from Eq. 1, it was linearized such that to plot a graph of $\ln\left(1 - \frac{[\mathrm{FF}]_t}{[\mathrm{FF}]_{\max}}\right)$ against t.

$$\ln\left(1 - \frac{[\mathrm{FF}]_t}{[\mathrm{FF}]_{\max}}\right) = -k_1 t\,. \quad (2)$$

In Eq. 2, $[\mathrm{FF}]_{\max}$ is the highest recorded constant concentration obtained at the maximum time specified for the reaction to take place. Hence, the slope of the straight linear plot is expected to give the value of k. For convenience, the rate constant for the specific reaction order is differentiated using a subscripted number. Herein, k_1 was made to represent the first-order case. In the second-order case, the rate of product formation depends on the square of the reactant concentration or a bimolecular interaction. Thus, the linearized version of the second-order rate (Eq. 3), i.e., Eq. 4, was employed to analyze the experimental data at all the temperatures studied. Lastly, the second-order rate, k_2, was determined by plotting $\frac{1}{[\mathrm{FF}]_t}$ against $\frac{1}{t}$.

$$[\mathrm{FF}]_t = \frac{[\mathrm{FF}]_{\max}^2 kt}{1 + [\mathrm{FF}]_{\max} kt}, \quad (3)$$

$$\frac{1}{[\mathrm{FF}]_t} = \frac{1}{k_2 t} + [\mathrm{FF}]_{\max}\,. \quad (4)$$

Ideally, Eqs. 1 and 3 for first- and second-order reaction rates were based on the conversion of pentosan into furfural, according to Reaction 5 [57], [105].

$$\mathrm{C_5H_{10}O_5} \xrightarrow{\mathrm{H_2SO_4,\ Heat}} \mathrm{C_5H_4O_2} + 3\mathrm{H_2O} \quad (5)$$

Indeed, furfural formation from potato peels is a chemical process, primarily involving acid hydrolysis of hemicelluloses (mainly pentosans, viz., 3.2–6.0% xylose) present in the peels [121], followed by their dehydration to form furfural, in accordance with Reaction 5 [122]. In this study, the possibility of side reactions, as noted by Mazar *et al.* [120], was ignored.

2.5. Thermodynamic computations

Changes in activation energy E_a, enthalpy ΔH, entropy ΔS, and Gibbs-Free energy ΔG occurring during the extraction, were determined using the Arrhenius expression (Eq. 6) [53], Eyring model (Eq. 7), as well as Eqs. 8 and 9, respectively.

$$\ln k_n = \ln k_0 - \frac{E_a}{R}\left(\frac{1}{T}\right), \quad (6)$$

$$k_n = k^* \frac{k_B T}{h} e^{\frac{\Delta G}{RT}}, \quad (7)$$

$$\ln \frac{k_n}{T} = \frac{-\Delta H}{R}\left(\frac{1}{T}\right) + \left(\ln k^* + \ln \frac{k_B}{h} + \frac{\Delta S}{R}\right), \quad (8)$$

$$\Delta G = \Delta H - T\Delta S, \quad (9)$$

wherein, E_a is the activation energy (kJ/mol); k_0 is the frequency factor; R = 8.314 J/(mol·K) is the universal gas constant; k^* is the transmission coefficient usually taken as 1; k_B is the Boltzmann constant = $1.38 \cdot 10^{-23}$ J/K; ΔH is the enthalpy change (kJ/mol); ΔS is the entropy change in kJ/(mol·K), n is the order of reaction (i.e., 1 or 2), and the Planck's constant $h = 6.63 \cdot 10^{-34}$ J·s = $1.842 \cdot 10^{-37}$ J·h. From a plot of ln k_n against $\frac{1}{T}$, k_0 was also determined, similar to the study undertaken by Eifert and Liauw [77]. Conversely, ΔH was computed from the slope of a plot of $\ln \frac{k_n}{T}$ against $\frac{1}{T}$ following the method adopted by Kim *et al.* [31]. For convenience, thermodynamic calculations were conducted for the order of reaction that best fit the furfural extraction data.

RESULTS AND DISCUSSION

3.1. Product concentration

At all temperatures, furfural concentration increases with time, indicating the progress of the acid-catalyzed dehydration reaction converting pentosans (from potato peels) to furfural. In this case, the temperature-dependent kinetic trends were consistent with reaction-controlled mechanisms rather than with diffusion-controlled ones, eliminating the need for the Thiele modulus or Weisz–Prater criterion confirmation. After reaching a certain point, the rate of increase slows down and stabilizes, which could indicate the equilibrium stage or the depletion of reactants. In Fig. 3, the concentration of furfural increases more rapidly, in accord with the findings of Uppal and Kaur [67], Kim *et al.* [31], and Liu *et al.* [94].

Higher temperatures accelerate the reaction rate due to increased molecular motion and collision frequency, as evident from the kinetics parameters where the rate constant k is higher at 80°C compared to 60 and 70°C. Specific behavior of the curve is observed at 60°C, where the reaction progresses slowly, reaching a lower maximum concentration over the same duration of 1–2 h compared to that at higher temperatures. However, at 70°C, the reaction is faster than at 60°C, with a steeper initial increase in furfural concentration and a higher maximum value, in line with the findings of Montanã *et al.* [34]. Eventually, the reaction achieves the highest maximum concentration at 80°C, over the shortest period of time, indicating an optimal conversion efficiency at this temperature, as shown in Fig. 3. As a clear deviation from the trend observed in Fig. 3, Xu *et al.* [124] showed that, along with an increase in time, furfural production declines rapidly at higher temperatures between 150–180°C. Based on the curve behavior in Fig. 3 and the data in Table 1, 80°C is recommended for furfural production. It offers the highest furfural yield in the shortest time frame (i.e., 0.56 g/cm^3), making it the most efficient temperature among those studied. However, such practical considerations as energy consumption and the potential for thermal degradation of furfural should be assessed before finalizing the process parameters. Previously, a significant furfural degradation under an increase in time was observed, when corncob was employed by Ji *et al.* [70].

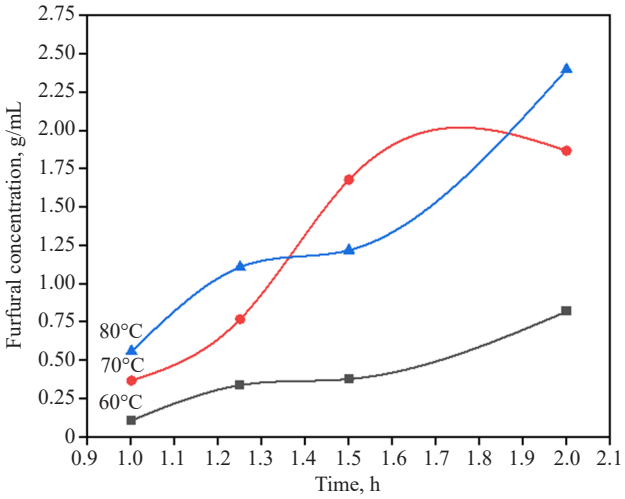

Fig. 3. Furfural concentration–time relationship at various temperatures

3.2. Kinetic study

Table 2 presents the furfural concentration at 60, 70, and 80°C over time, along with the data relevant to first-order and second-order reaction kinetics. As mentioned earlier, at higher temperatures (70 and 80°C), furfural concentrations increase more rapidly and achieve higher values, reflecting faster reaction rates and greater product yields as compared to those at 60°C.

Table 2. Concentration of furfural and representative kinetic plot data

t, h	$[FF]_t$, g/mL	$\frac{[FF]_t}{[FF]_{max}}$	$1-\frac{[FF]_t}{[FF]_{max}}$	$\ln\left(1-\frac{[FF]_t}{[FF]_{max}}\right)$	$\frac{1}{[FF]_t}$, mL/g
60°C					
1.00	0.11	0.134146341	0.865853659	−0.144039370	9.090909
1.25	0.34	0.414634146	0.585365854	−0.535518236	2.941176
1.50	0.38	0.463414634	0.536585366	−0.622529613	2.631579
2.00	0.82	1	0	–	1.219512
70°C					
1.00	0.37	0.451219512	0.548780488	−0.600056757	2.702703
1.25	0.77	0.939024390	0.060975610	−2.797281335	1.298701
1.50	1.68	2.048780488	−1.048780488	–	0.595238
2.00	1.87	2.280487805	−1.280487805	–	0.534759
80°C					
1.00	0.56	0.682926829	0.317073171	−1.148622709	1.785714
1.25	1.11	1.353658537	−0.353658537	–	0.900901
1.50	1.22	1.487804878	−0.487804878	–	0.819672
2.00	2.40	2.926829268	−1.926829268	–	0.416667

The term inside the logarithm, $1-\frac{[FF]_t}{[FF]_{max}}$, depends on the ratio of the furfural concentration at time, t, $[FF]_t$, to the maximum concentration, $[FF]_{max}$. As the reaction progresses and $[FF]_t$ approaches $[FF]_{max}$, the expression $1-\frac{[FF]_t}{[FF]_{max}}$ approaches zero. The logarithm of zero is undefined; therefore, this term cannot be calculated and is marked with a dash ('–') in Table 2. The increasing number of dashes with temperature progression ('1' at 60°C, '2' at 70°C, '3' at 80°C) highlights the influence of higher temperatures on reaction kinetics, bringing the system closer to equilibrium faster, which subsequently impacts the logarithmic calculations in the data table. This pattern of dashes confirms the temperature-dependent kinetics of furfural production, with 80°C being the most efficient temperature for achieving the maximum concentration rapidly. Xia *et al.* [84] reported a low furfural generation at this temperature during furfural synthesis from bamboo and xylose.

3.2.1. First-order reaction

A straight-line trend in Figs. 4a and 4b agrees well with the theoretical prediction of Eq. 2 (first-order furfural product formulation); however, the reaction may involve secondary processes which affect the data slightly. The coefficient of determination (R^2) = 0.8811 at 60°C in Fig. 4a indicates a reasonably good fit to the first-order model and suggests that the reaction at this temperature moderately follows first-order kinetics. At the same time, some deviations from linearity might exist (Fig. 4b). The near-perfect linear relationship between $\ln\left(1-\frac{[FF]_t}{[FF]_{max}}\right)$ and time (i.e., R^2 = 1) implied that the reaction at 70°C is predominantly governed by the first-order rate law, above other temperatures examined. In Fig. 4c, the plot shows only one data point, which is insufficient to establish a linear trend or calculate an R^2 value reliably.

The single data point at 80°C (−1.149 when t = 1 h) highlights the challenge of collecting sufficient data for kinetic modeling when reactions proceed rapidly to equilibrium. Nonetheless, the overall trend supports the applicability of the first-order model to describe the reaction, in particular, at intermediate temperatures of about 70°C.

3.2.2. Second-order reaction

Rate plots in Fig. 5 were constructed to test the relationship between $\frac{1}{[FF]_t}$ and $\frac{1}{t}$ as well as to evaluate the correspondence of the experimental data with the second-order model. The R^2 values progress

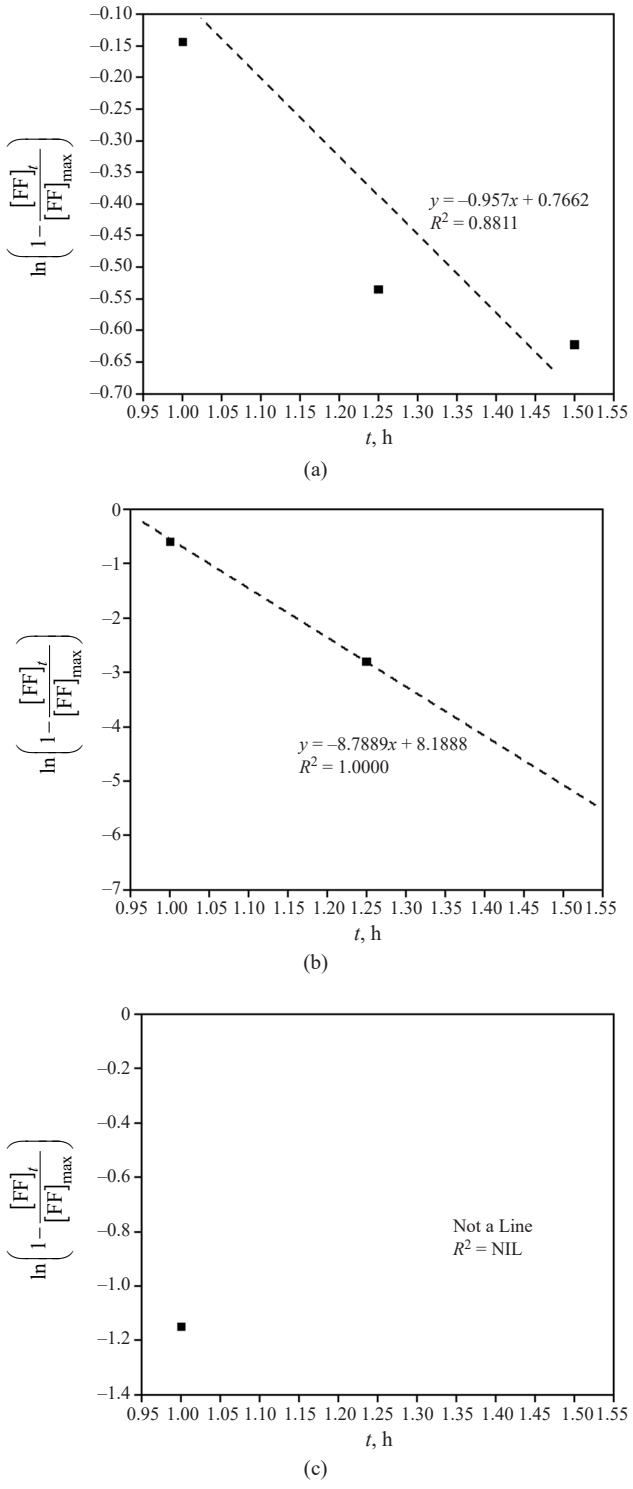

Fig. 4. Rate plots for the first-order furfural formation at (a) 60, (b) 70, and (c) 80°C

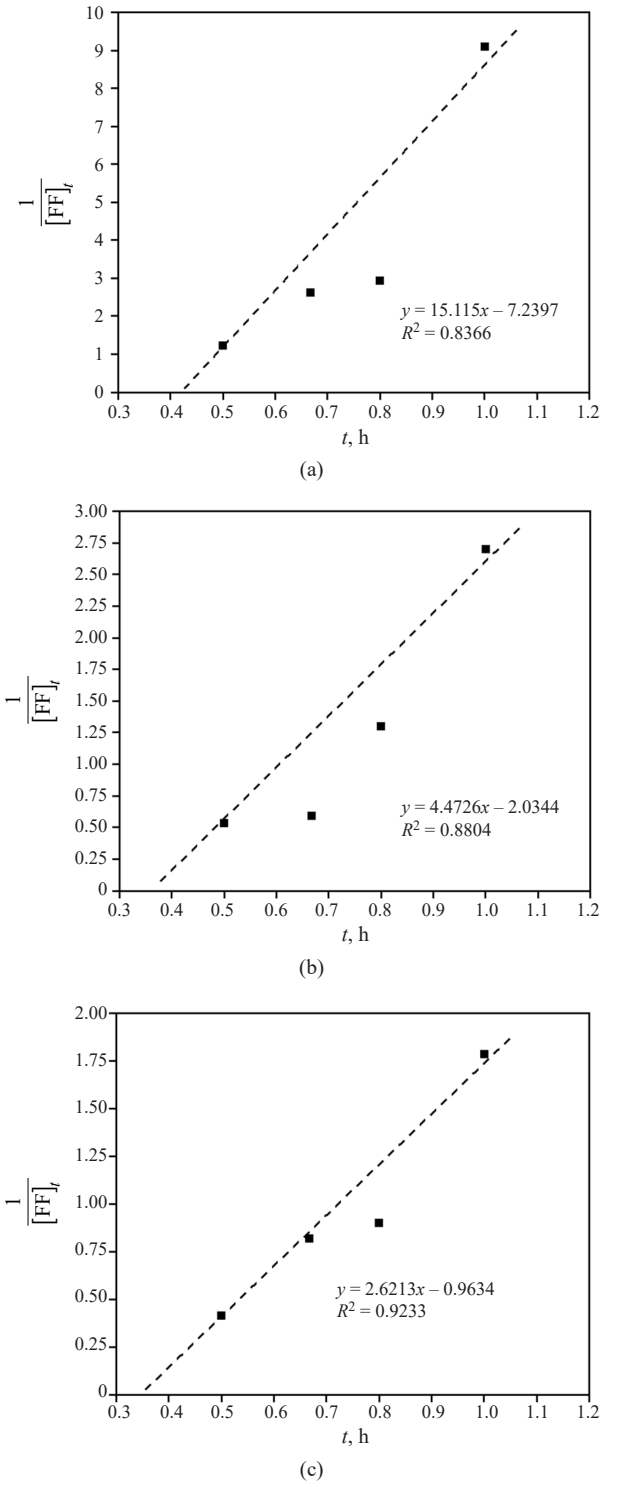

Fig. 5. Rate plots for the second-order furfural formation at (a) 60, (b) 70, and (c) 80°C

from 0.8366 at 60°C to 0.9233 at 80°C, reflecting that the reaction kinetics adhere more strongly to the second-order model at higher temperatures. This trend suggests that temperature plays a critical role in enhancing the applicability of the second-order kinetics in describing furfural formation.

The extraction data align more closely with the first-order assumptions at lower and intermediate temperatures (60 and 70°C), since the straight-line trends in Fig. 4 have better fits (R^2 values) to the first-order rate law. At 80°C, the second-order model shows a stronger fit, possibly due to temperature-induced changes in reaction

dynamics. However, the first-order model remains the overall better descriptor of the reaction kinetics across the temperature range studied.

3.2.3. Estimated kinetic parameters

It is well known that k unit depends on the order of reaction. As such, the terminology 'units' would be use for appropriateness. The increase in k with temperature for both the first-order and second-order reactions, as shown in Table 3, can be explained by the fundamental principles of chemical kinetics, particularly the Arrhenius equation and the temperature dependence of reaction rates. Reasons for this increase of k with temperature are due to enhanced molecular energy, exponential relationship and increased reaction rates.

Table 3. Calculated first- and second-order kinetic constants

Reaction order	Temperature, °C	Slope	k, units	R^2
1	60	−0.9570	0.9570	0.8811
	70	−8.7889	8.7889	1.0000
	80	–	–	
2	60	15.1150	0.066159	0.8366
	70	4.4726	0.223584	0.8804
	80	2.6213	0.381490	0.9233

As temperature increases, molecules gain kinetic energy, leading to more frequent and energetic collisions between the reactants. It results in a higher proportion of molecules having sufficient energy to overcome the activation energy barrier (E_a). The Arrhenius equation shows an exponential dependence of k on T. Even an insignificant increase in temperature can significantly enhance the rate constant due to the exponential term. And at higher temperatures, the reaction progresses more rapidly, reflected in the larger values of k for both first-order (8.7889) and second-order reactions (0.3815). In the first-order model, k increases from 0.957 at 60°C to 8.7889 at 70°C, indicating a dramatic rise in the reaction rate with a modest temperature increase. In the second-order model, the rise in k is less steep compared to the first-order reaction, reflecting differences in the response of the reaction mechanism to temperature changes. Generally, at n = 1, the reaction rate depends linearly on the concentration of one reactant; hence, k increases more sharply with temperature due to its direct effect on the formation rate of furfural. However, at n = 2, the rate depends on the square of the reactant concentration or a bimolecular interaction, leading to a more moderate increase in k with temperature.

3.3. Thermodynamic study

Equations 6 and 8 were key to finding the thermodynamic energy parameters of the solvent extraction process, through the calculated data in Table 4. The rate constant, k_1, reflects the reaction speed. At 70°C, the reaction rate is significantly higher compared to 60°C, resulting in a higher value of k_1.

Table 4. Axis data for straight-line plots for energy parameter determination

T, °C	T, K	k_1, h^{-1}	$\frac{1}{T}$, $\frac{1}{\text{K}}$	ln k_1	$\ln\frac{k_1}{T}$
		n = 1			
60	333.15	0.9570	0.003002	−0.04395	−5.85254
70	343.15	8.7889	0.002914	2.17349	−3.66468
80	353.15	–	–	–	–
T, °C	T, K	k_2, units	$\frac{1}{T}$, $\frac{1}{\text{K}}$	ln k_2	$\ln\frac{k_2}{T}$
		n = 2			
60	333.15	0.066159	0.003002	−2.71569	−8.52429
70	343.15	0.223584	0.002914	−1.49797	−7.33614
80	353.15	0.381490	0.002832	−0.96367	−6.83056

Ln k_1 is the natural logarithm of the rate constant k_1. For k_1 values greater than 1 (as observed at 70°C for the first-order reaction), ln k_1 becomes positive. The 70°C temperature likely represents an optimal point where the reaction proceeds efficiently without the limitations observed at lower (a slower reaction) or higher temperatures (equilibrium reached too rapidly). This results in a k_1 value sufficiently large to make ln k_1 positive (at 2.1735). Figures 6 and 7 displays the Arrhenius plot as well as the Eyring model plot described earlier for the two reaction rates. To determine which thermodynamic plot provides the best fit and supports a particular order of reaction, the fit quality (e.g., linearity and R^2 values) and trends in Figs. 6 and 7 should be analyzed. The fit quality or linearity as well as R^2 values of unity aligned best with the furfural experimental data for first-order Arrhenius and Eyring-Polanyi models, as observed in Fig. 6. However, it appears less linear in the second-order case shown in Fig. 7 with a lower average R^2 value of 0.9573.

While both the first- and second-order models show reasonable fits, the first-order thermodynamic plots (Figs. 6a and 6b) provide the best overall fit, making the first-order reaction the most plausible mechanism for the extraction process under the conditions studied. Through simplification of Eq. 8, ΔS was calculated using Eq. 10,

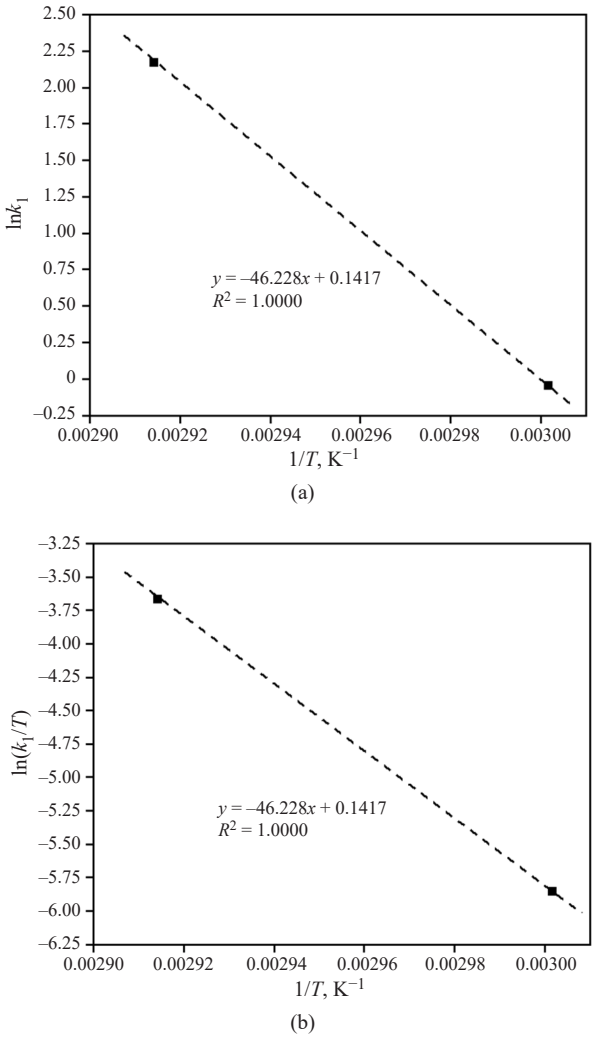

Fig. 6. First-order thermodynamic plots: (a) Arrhenius and (b) Eyring models

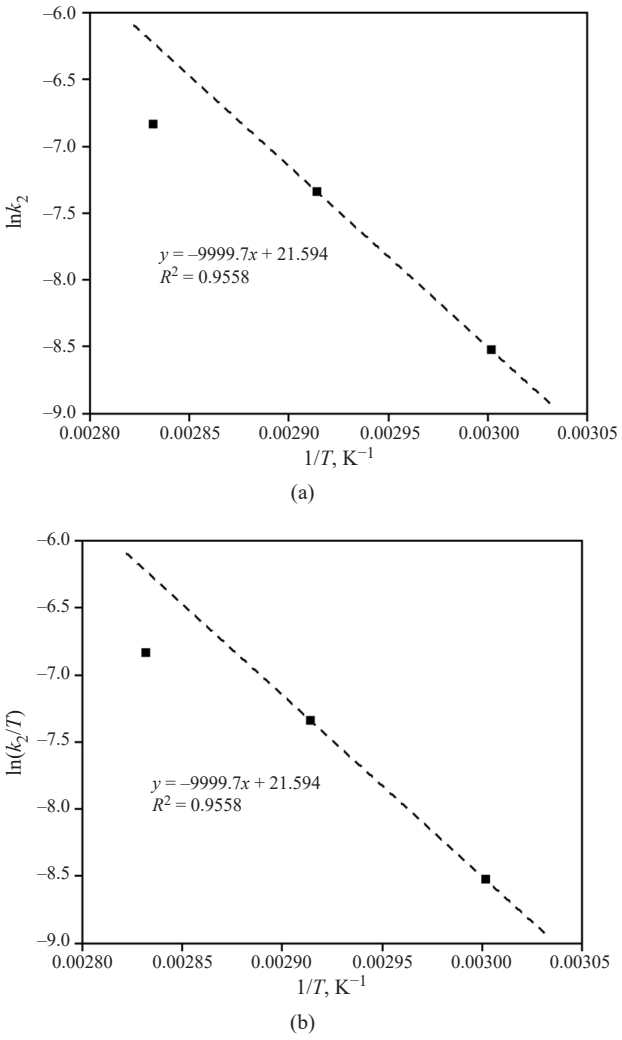

Fig. 7. Second-order thermodynamic plots: (a) Arrhenius and (b) Eyring models

by substituting the known constant values and the intercept in Fig. 6b.

$$31.9476 + \frac{\Delta S}{R} = \text{Intercept.} \quad (10)$$

The higher E_a = 85.992 kJ/mol for the first-order reaction indicates a higher energy barrier for the reaction to occur. By implication, the first-order reaction requires a greater energy input to initiate compared to the second-order reaction, potentially making it slower at lower temperatures. Both E_a are by far < 115 kJ/mol obtained by Liu *et al.* [30] who utilized hardwood PHL for furfural manufacture, although being > 28.69 and 34.72 kJ/mol realized by Xu *et al.* [123]. Provided that this high energy requirement is approved, potato peel has the potential to add to the existing global furfural tonnage, whose expected compound annual growth rate equals 6.5% [124]. Likewise, the higher ΔH = 83.138 kJ/mol in the first-order reaction compared to the second-order version implies its more endothermic character, thus requiring a greater energy input to proceed. Thus, it aligns with its higher observed E_a in Table 5. In contrast, the higher first-order k_0 > 4.77 units in the second-order reaction signifies a greater likelihood of successful collisions leading to furfural product formation. It indicates that while the energy barrier is higher, the reaction has a stronger dependence on the frequency of molecular collisions.

Table 5. Energy parameters computed for both reaction orders

Parameter	First-order	Second-order
E_a, J/mol	85991.702	4822.951
k_0, units	$2.22549 \cdot 10^{12}$	4.773119
ΔH, J/mol	83137.5058	1972.081
ΔS, J/mol·K	−86.0798304	−309.467
ΔG at 333 K, J/mol	111802.0893	105024.6
ΔG at 343 K, J/mol	112662.8876	108119.3
ΔG at 353 K, J/mol	–	111213.9

A less negative ΔS for the first-order reaction suggests a smaller decrease in the system disorder during the reaction, which could indicate a more favorable pathway compared to the second-order reaction. However, the higher ΔG values for the first-order reaction at all temperatures suggest its being less thermodynamically favorable than the second-order reaction. Lower ΔG values for the second-order reaction, as illustrated in Fig. 8, implied its more spontaneous character. In a nutshell, for $n = 1$, the high E_a, ΔH, and ΔG indicate that while it is less spontaneous and more energy-intensive, it may offer greater control and predictability under optimized conditions. On the other hand, for $n = 2$, the lower E_a, ΔH, and ΔG specify that it is less energy-demanding and more thermodynamically favorable, making it potentially more efficient under practical conditions.

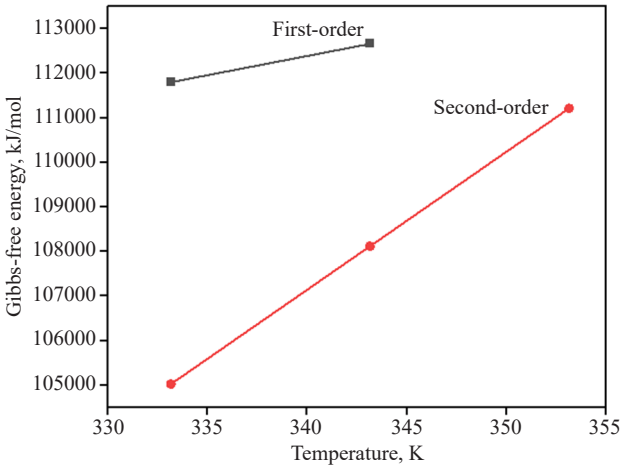

Fig. 8. Effect of temperature change on Gibbs energy

Hence, the second-order reaction can be recommended for the extraction of furfural from potato peels due to its lower energy and thermodynamic barriers, indicating its greater efficiency and practicality for large-scale applications. However, the first-order reaction might be selected in cases where precise reaction control and selectivity are critical.

CONCLUSIONS

Furfural, regarded as "the sleeping beauty of bio-renewable chemicals," was successfully produced via the acid-catalyzed hydrolysis technique over the time interval of 1–2 h, separately at 60, 70, and 80°C. Optimal extraction was achieved at 80°C, ensuring the highest furfural yield within the shortest duration of 2 h. The first-order reaction kinetic mechanism was shown to be the primary pathway under most conditions given its perfect fit ($R^2 = 1$) at 70°C and $k_1 = 8.7889$ min^{-1}. Thermodynamic analyses indicated that while the second-order reaction displayed lower energy and entropic barriers, the first-order reaction offered greater precision in modeling the process. Thus, utilization of sweet potato peels as feedstock not only provides a cost-effective alternative but also promotes the valorization of agricultural waste, aligning with global efforts toward circular economy practices. The use of dichloromethane and the effectiveness of sulfuric acid as a catalyst attest to the potential of sweet potato peels for appreciable extraction of furfural. Future work should explore the integration of greener solvents and advanced separation techniques to further improve furfural purity and energy efficiency. Scaling this process to industrial applications could significantly contribute to meeting the growing demand for bio-renewable chemicals, thus fostering a sustainable chemical industry. The utilization of Aspen Plus to simulate the efficiency of solvent recovery and to assess large-scale applicability is recommended. Purification of the extracted furfural by fractional distillation appears beneficial, although only when necessary.

Authors' contributions

Abdulhalim Musa Abubakar conceived and supervised the study,

Iyisikwe Tanimu Umar contributed to experimental design and data collection,

Abass-Giwa Muhammed Akintunde handled data analysis and interpretation,

Muhammad Jimada Aliyu provided technical validation and review,

Marwea Al-Hedrewy offered international collaboration and critical insights, and

Uday Raheja assisted in manuscript writing and editing.

REFERENCES

1. Rachamontree P., Douzou T., Cheenkachorn K., Sriariyanun M., Rattanaporn K. Furfural: A sustainable platform chemical and fuel. *Appl. Sci. Eng. Prog.* 2020;13(1):3–10. https://doi.org/10.14416/j.asep.2020.01.003
2. Win D.T. Furfural–Gold from garbage. *Assumpt. Univ. J. Technol.* (*AU J.T.*). 2005;8(4):185–190. Available: https://www.thaiscience.info/Journals/Article/AUJT/10290551.pdf. Accessed January 5, 2025.
3. Nagaraju T V., Rao M V., Sunil B. M., Chaudhary B. Furfural-extracted corncob ash: A new geomaterial for sustainable construction. In: Hazarika H., Haigh S.K., Chaudhary B., Murai M., Manandhar S. (Eds.). *Sustainable Construction Resources in Geotechnical Engineering* (*IC-CREST 2023*). *Lecture Notes in Civil Engineering*. Singapore: Springer, 2024. V. 448. P. 155–162. https://doi.org/10.1007/978-981-99-9227-0_15

4. Kabbour M., Luque R. Furfural as a platform chemical: from production to applications. In: *Recent Advances in Development of Platform Chemicals*. Elsevier B.V.; 2020. Ch. 10. P. 283–297. https://doi.org/10.1016/B978-0-444-64307-0.00010-X
5. Madloom A.A., Jabbar S.M., Kadhim N.J. Furfural production based cellulosic garbage. *Plant Arch.* 2019;19(2):345–350. Available: https://www.plantarchives.org/SPL%20ISSUE%20SUPP%202,2019/63%20(345-350).pdf. Accessed January 5, 2025.
6. Garcıa-Domınguez M.T., Garcıa-Domınguez J.C., Lopez F., De Diego C.M., Diaz M.J. Maximizing furfural concentration from wheat straw and Eucalyptus globulus by nonisothermal autohydrolysis. *Environ. Prog. Sustain. Energy*. 2015;34(K):1236–1242. https://doi.org/10.1002/ep.12099
7. Yong T.L.-K., Mohamad N., Yusof N.N.M. Furfural production from oil palm biomass using a biomass-derived supercritical ethanol solvent and formic acid catalyst. *Procedia Eng.* 2016;148:392–400. https://doi.org/10.1016/j.proeng.2016.06.495
8. Eseyin A.E., Steele P.H. An overview of the applications of furfural and its derivatives. *Int. J. Adv. Chem.* 2015;3(2):42–47. https://doi.org/10.14419/ijac.v3i2.5048
9. Brazdausks P., Puke M., Vedernikovs N., Kruma I. Influence of biomass pretreatment process time on furfural extraction from birch wood. *Environ. Clim. Technol.* 2013;11:5–11. https://doi.org/10.2478/rtuect-2013-0001
10. Gebre H., Fisha K., Kindeya T., Gebremicha T. Synthesis of furfural from bagasse. *Int. Lett. Chem. Phys. Astron.* 2015;57:72–84. https://doi.org/10.56431/p-5301hc, https://doi.org/10.18052/www.scipress.com/ILCPA.57.72
11. Yahyazadeh A. Extraction and investigation of furfural in tea leaves and comparing with furfural in rice hull. *J. Pharm. Res.* 2011;4(12):4338–4339. Available: https://www.jpronline.info. Accessed January 5, 2025.
12. Croker J.R. *The Production of Furfural from Agricultural Waste in Australia*: Masters Thesis. Degree of Master of Science in Food Technology. School of Food Technology, University of New South Wales. 1983. 139 p. https://doi.org/10.26190/unsworks/5665
13. Clauser N.M., Area M.C., Felissia F.E., Vallejos M.E. Techno-economic assessment of carbonyxlic acids, furfural, and pellet production in a pine sawdust biorefinery. *Biofuels Bioprod. Biorefining*. 2018;12(6):997–1012. https://doi.org/10.1002/bbb.1915
14. Luo A.Y., Li Z., Li X., *et al.* The production of furfural directly from hemicellulose in lignocellulosic biomass: A review. *Catal. Today*. 2018;319:14–24. https://doi.org/10.1016/j.cattod.2018.06.042
15. Gürbüz E.I., Gallo J.M.R., Alonso D.M., Wettstein S.G., Lim W.Y., Dumesic J.A. Conversion of hemicellulose into furfural using solid acid catalysts in γ -Valerolactone. *Angew. Chem. Int. Ed. Zuschriften*. 2013;52(4):1270–1274. https://doi.org/10.1002/anie.201207334
16. Agirrezabal-Telleria I., Gandarias I., Arias P.L. Production of furfural from pentosan-rich biomass: Analysis of process parameters during simultaneous furfural stripping. *Bioresour. Technol.* 2013;143:258–264. https://doi.org/10.1016/j.biortech.2013.05.082
17. Nunez F., Sumoza D., Garcia F., Rosales C., Jhonny J.M.B. Recovery and characterization of furfural obtained from rice husk. *Ciencia en Revoluc.* 2021;7(22):121–127. https://doi.org/10.5281/zenodo.6429799
18. Riera F.A., Alvarez R., Coca J. Production of furfural by acid hydrolysis of corncobs. *J. Chem. Technol. Biotechnol.* 1991;50(2):149–155. https://doi.org/10.1002/jctb.280500202
19. Peleteiro S., Rivas S., Alonso J.L., Santos V., Parajó J.C. Furfural production using ionic liquids: A review. *Bioresour. Technol.* 2016;202:181–191. https://doi.org/10.1016/j.biortech.2015.12.017
20. Zhao Y., Xu H., Wang K., *et al.* Enhanced furfural production from biomass and its derived carbohydrates in renewable butanone–water solvent system. *Sustain. Energy Fuels*. 2019;3(11):3208–3218. https://doi.org/10.1039/C9SE00459A
21. Mao L., Zhang L., Gao N., Li A. $FeCl_3$ and acetic acid co-catalyzed hydrolysis of corncob for improving furfural production and lignin removal from residue. *Bioresour. Technol.* 2012;123:324–331. https://doi.org/10.1016/j.biortech.2012.07.058
22. Li X.-K., Fang Z., Luo J., Su T.-C. Co-production of furfural and easily hydrolysable residue from sugarcane bagasse in MTHF/aqueous biphasic system: influence of acid species, NaCl addition and MTHF. *ACS Sustain. Chem. Eng.* 2016;4(10):5804–5813. https://doi.org/10.1021/acssuschemeng.6b01847
23. Martín M., Grossmann I.E. Optimal production of furfural and DMF from algae and switchgrass. *Ind. Eng. Chem. Res.* 2016;55(12):3192–3202. https://doi.org/10.1021/acs.iecr.5b03038
24. Bhaumik P., Dhepe P.L. Exceptionally high yields of furfural from assorted raw biomass over solid acids. *RSC Adv.* 2014;4(50):26215–26221. https://doi.org/10.1039/c4ra04119d
25. Ji H., Chen L., Zhu J., Gleisner R., Zhang X. Reaction kinetics based optimization of furfural production from corncob using a fully recyclable solid acid. *Ind. Eng. Chem. Res.* 2016;55(43):11253–11259. https://doi.org/10.1021/acs.iecr.6b03243
26. Chen H., Qin L., Yu B. Furfural production from steam explosion liquor of rice straw by solid acid catalysts (HZSM-5). *Biomass and Bioenergy*. 2014;73:77–83. https://doi.org/10.1016/j.biombioe.2014.12.013
27. Gallo J.M.R., Alonso D.M., Mellmer M.A., Yeap J.H., Wong H.C., Dumesic J.A. Production of furfural from lignocellulosic biomass using beta zeolite and biomass-derived solvent. *Top Catal*. 2013;56(18–20):1774–1781. https://doi.org/10.1007/s11244-013-0113-3
28. Liu F., Boissou F., Vignault A., *et al.* Conversion of wheat straw to furfural and levulinic acid in a concentrated aqueous solution of betaıne hydrochloride. *RSC Adv.* 2014;4(55):28836–28841. https://doi.org/10.1039/C4RA03878A
29. Delbecq F., Wang Y., Len C. Conversion of xylose, xylan and rice husk into furfural via betaine and formic acid mixture as novel homogeneous catalyst in biphasic system by microwave-assisted dehydration. *J. Mol. Catal. A Chem.* 2016;423:520–525. https://doi.org/10.1016/j.molcata.2016.07.003
30. Liu H., Hu H., Baktash M.M., Jahan M.S., Ahsan L., Ni Y. Kinetics of furfural production from pre-hydrolysis liquor (PHL) of a kraft-based hardwood dissolving pulp production process. *Biomass and Bioenergy*. 2014;66:320–327. https://doi.org/10.1016/j.biombioe.2014.02.003
31. Kim E.S., Liu S., Abu-Omar M.M., Mosier N.S. Selective conversion of biomass hemicellulose to furfural using maleic acid with microwave heating. *Energy Fuels*. 2012;26(2):1298−1304. https://doi.org/10.1021/ef2014106
32. Yemis O., Mazza G. Optimization of furfural and 5-hydroxymethylfurfural production from wheat straw by a microwave-assisted process. *Bioresour. Technol.* 2012;109:215–223. https://doi.org/10.1016/j.biortech.2012.01.031
33. Mandalika A.S., Runge T.M. Improved method of producing furfural from biomass. In: *Conf. Dallas, Texas, July 29 – August 1, 2012*. 2012. 121337810. http://doi.org/10.13031/2013.41836

34. Montanã D., Salvadã J., Torras C., Farriol X. High-temperature dilute-acid hydrolysis of olive stones for furfural production. *Biomass and Bioenergy*. 2002;22(4): 295–304. https://doi.org/10.1016/S0961-9534(02)00007-7
35. Weidener D., Leitner W., De Maria P.D., Klose H., Grande P.M. Lignocellulose fractionation using recyclable phosphoric acid: Lignin, cellulose and furfural production. *ChemSusChem.* 2020;14(3):909–916. https://doi.org/10.1002/cssc.202002383
36. Sanchez V., Dafinov A., Salagre P., Llorca J., Cesteros Y. Microwave-assisted furfural production using hectorites and fluorohectorites as catalysts. *Catalysts*. 2019;9(9):706. https://doi.org/10.3390/catal9090706
37. Fan B., Kong L., He Y. Highly efficient production of furfural from corncob by barley hull biochar-based solid acid in cyclopentyl methyl ether–water system. *Catalysts*. 2024;14(9):583. https://doi.org/10.3390/catal14090583
38. Bao Y., Du Z., Liu X., *et al.* Furfural production from lignocellulosic biomass: one-step and two-step strategies and techno-economic evaluation. *Green Chem.* 2024;26(11): 6318–6338. https://doi.org/10.1039/D4GC00883A
39. Zhao Y., Lu K., Xu H., Zhu L., Wang S. A critical review of recent advances in the production of furfural and 5-hydroxymethylfurfural from lignocellulosic biomass through homogeneous catalytic hydrothermal conversion. *Renew. Sustain. Energy Rev.* 2021;139:110706. https://doi.org/10.1016/j.rser.2021.110706
40. Zhang T., Li W., Xiao H., Jin Y., Wu S. Recent progress in direct production of furfural from lignocellulosic residues and hemicellulose. *Bioresour. Technol.* 2022;354:127126. https://doi.org/10.1016/j.biortech.2022.127126
41. Yong K.J., Wu T.Y., Lee C.B.T.L., *et al.* Furfural production from biomass residues: Current technologies, challenges and future prospects. *Biomass and Bioenergy*. 2022;161:106458. https://doi.org/10.1016/j.biombioe.2022.106458
42. Muryanto M., Sudiyani Y., Harahap A.F.P., Gozan M. Furfural and derivatives from bagasse and corncob. In: Abd-Aziz S., Gozan M., Ibrahim M.F., Phang L.-Y. (Eds.). *Chemical Substitutes from Agricultural and Industrial By-Products: Bioconversion, Bioprocessing, and Biorefining*. 2023. Ch. 14. P. 279–300. https://doi.org/10.1002/9783527841141.ch14
43. Lee C.B.T.L. and Wu T.Y. A review on solvent systems for furfural production from lignocellulosic biomass. *Renew. Sustain. Energy Rev.* 2020;137:110172. https://doi.org/10.1016/j.rser.2020.110172
44. Zhang X., Zhu P., Li Q., Xia H. Recent advances in the catalytic conversion of biomass to furfural in deep eutectic solvents. *Front. Chem.* 2022;10:911674. https://doi.org/10.3389/fchem.2022.911674
45. Mohamad N., Abd-Talib N., Yong T.-L.K. Furfural production from oil palm frond (OPF) under subcritical ethanol conditions. *Mater. Today Proc.* 2020;31(Part 1):116–121. https://doi.org/10.1016/j.matpr.2020.01.256
46. Raman J.K. and Gnansounou E. Furfural production from empty fruit bunch–A biorefinery approach. *Ind. Crops Prod.* 2015;69:371–377. https://doi.org/10.1016/j.indcrop.2015.02.063
47. Qatrunnada A., Muryanto M., Darmawan M.A., Gozan M. Optimization of furfural liquid-liquid extraction from oil palm empty fruit bunch hydrolysate solution with solvent variations. *AIP Conf. Proc*. 2024;3080(1):050002. (*The 15th Asian Congress on Biotechnology in conjunction with the 7th International Symposium on Biomedical Engineering* (*ACB-ISBE 2022*)). https://doi.org/10.1063/5.0198973
48. Othman N.E.A., Abd Aziz A., Wan Hassan W.H., Jailani N.F., Abd Hamid F., Abdul Wahab N. Production of furfural from oil palm fibres. *J. Oil Palm Res.* 2020;33(3): 473–481. Available: http://jopr.mpob.gov.my/. Accessed January 5, 2025.
49. Tareen A.K., Punsuvon V., Parakulsuksatid P. Conversion of steam exploded hydrolyzate of oil palm trunk to furfural by using sulfuric acid , solid acid, and base catalysts in one pot. *Energy Sources, Part A: Recover. Util. Environ. Eff.* 2020;46(1): 6126-6137. https://doi.org/10.1080/15567036.2020.1741733
50. García-Domínguez M.T., García-Domínguez J.C., Feria M.J., Gómez-Lozano D.M., López F., Díaz M.J. Furfural production from Eucalyptus *globulus*: Optimizing by using neural fuzzy models. *Chem. Eng. J.* 2013;221:185–192. https://doi.org/10.1016/j.cej.2013.01.099
51. López F., *et al.* Optimization of furfural production by acid hydrolysis of Eucalyptus *globulus* in two stages. *Chem. Eng. J.* 2014;240:195–201. https://doi.org/10.1016/j.cej.2013.11.073
52. Padilla-Rascón C., Romero-García J.M., Ruiz E., Romero I., Castro E. Microwave-assisted production of furfural from the hemicellulosic fraction of olive stones. *Process Saf. Environ. Prot.* 2021;152:630–640. https://doi.org/10.1016/j.psep.2021.06.035
53. Rivas S., Vila C., Santos V., Parajó J.C. Furfural production from birch hemicelluloses by two-step processing: a potential technology for biorefineries. *Holzforschung*. 2016;70(10): 901–910. https://doi.org/10.1515/hf-2015-0255
54. Brazdausks P., Puke M., Vedernikovs N., Irçna K. The effect of catalyst amount on the production of furfural and acetic acid from birch wood in a biomass pretreatment process. *Baltic Forestry.* 2014;20(1):106–114. Available: https://ortus.rtu.lv/science/en/publications/18956. Accessed January 5, 2025.
55. Brazdausks P., Vedernikovs N., Puke M., Kruma I. Effect of the acid hydrolysis temperature on the conversion of birch wood hemicelluloses into furfural. *Key Eng. Mater.* 2014;604: 245–248. https://doi.org/10.4028/www.scientific.net/KEM.604.245
56. García M.T., Zamudio M.A.M., Loaiza J.M., *et al.* Characterization and use of southern cattail for biorefining-based production of furfural. *Biomass Convers. Bioref.* 2019;9:333–339. https://doi.org/10.1007/s13399-018-0355-1
57. Kazemi M., Zand-Monfared M.R. Furfural production from pisthachio green hulls as agricultural residues. *J. Appl. Chem. Res.* 2010;3(12):19–24. Available: http://www.sid.ir/. URL: https://citeseerx.ist.psu.edu/document?repid=rep1&type=pdf&doi=a614365d06f93de64cb2c2345fe3855f7824b198. Accessed January 5, 2025.
58. Yue Z., Sun L.-L., Sun S.-N., Cao X.-F., Wen J.-L., Zhu M.-Q. Structure of corn bran hemicelluloses isolated with aqueous ethanol solutions and their potential to produce furfural. *Carbohydr. Polym.* 2022;288:119420. https://doi.org/10.1016/j.carbpol.2022.119420
59. Mao L., Zhang L., Gao N., Li A. Seawater based furfural production via corncob hydrolysis catalyzed by $FeCl_3$ in acetic acid steam. *Green Chem.* 2013;15(3):727–737. https://doi.org/10.1039/C2GC36346A
60. Barbosa B.M., Colodette J.L., Junior D.L., Gomes F.J.B., Martino D.C. Preliminary studies on furfural production from lignocellulosics. *J. Wood Chem. Technol.* 2014;34(3):37–41. https://doi.org/10.1080/02773813.2013.844167
61. Soludongwe S.M. Co-production of furfural and wood composite products from bio-based processing residues: Thesis for Degree of Master of Agricultural Sciences. Faculty of AgriSciences, Stellenbosch University. 2020. Available: https://scholar.sun.ac.za. Accessed January 5, 2025.

62. Bariani M., Boix E., Cassella F., Cabrera M.N. Furfural production from rice husks within a biorefinery framework. *Biomass Convers. Bioref.* 2021;11:781–794. https://doi.org/10.1007/s13399-020-00810-1
63. Sashikala M., Ong H.K. Synthesis and identification of furfural from rice straw. *J. Trop. Agric. Food Sci.* 2007;35(1):165–172. Available: https://jtafs.mardi.gov.my/jtafs/35-1/Furfural.pdf. Accessed January 5, 2025.
64. Sashikala M., Ong H.K. Synthesis, identification and evaluation of furfural from rice straw. *J. Trop. Agric. Food Sci.* 2009;37(1):95–101. Available: https://www.cabidigitallibrary.org/doi/pdf/10.5555/20113329392. Accessed January 5, 2025.
65. Singh A., Das K., Sharmab D.K. Production of xylose, furfural, fermentable sugars and ethanol from agricultural residues. *J. Chem. Technol. Biotechnol.* 1984;34(2):51–61. https://doi.org/10.1002/jctb.5040340203
66. Uppal S.K., Gupta R., Dhillon R.S., Bhatia S. Potential of sugarcane bagasse for production of furfural and its derivatives. *Sugar Tech*. 2009;10(4):298–301. http://doi.org/10.1007/s12355-008-0053-6
67. Uppal S.K., Kaur R. Hemicellulosic furfural production from sugarcane bagasse using different acids. *Sugar Tech*. 2011;13(2):166–169. https://doi.org/10.1007/s12355-011-0081-5
68. Wang Q., Zhuang X., Wang W., Tan X., Yu Q., Qi W. Rapid and simultaneous production of furfural and cellulose-rich residue from sugarcane bagasse using a pressurized phosphoric acid-acetone-water system. *Chem. Eng. J.* 2017;334:698–706. https://doi.org/10.1016/j.cej.2017.10.089
69. Gomes G.R., Scopel E., Breitkreitz M.C., Rezende C.A., Pastre J.C. Valorization of sugarcane bagasse C5-fraction by furfural production mediated by renewable glycine-based ionic liquid. *Ind. Crops Prod.* 2022;191(Part A):115940. https://doi.org/10.1016/j.indcrop.2022.115940
70. Ji H., Zhu J.Y., Gleisner R. Integrated production of furfural and levulinic acid from corncob in a one-pot batch reaction incorporating distillation using step temperature profiling. *RSC Adv.* 2017:7(73):46208–46214. https://doi.org/10.1039/c7ra08818c
71. Ren J., Wang W., Yan Y., Deng A., Chen Q., Zhao L. Microwave-assisted hydrothermal treatment of corncob using tin(IV) chloride as catalyst for furfural production. *Cellulose*. 2016;23(3):1649–1661. https://doi.org/10.1007/s10570-016-0898-x
72. Wang Q., *et al.* Production of furfural with high yields from corncob under extremely low water/solid ratios. *Renew. Energy*. 2019;144:139–146. https://doi.org/10.1016/j.renene.2018.07.095
73. Bu L., Tang Y., Gao Y., Jian H., Jiang J. Comparative characterization of milled wood lignin from furfural residues and corncob. *Chem. Eng. J.* 2011;175:176–184. https://doi.org/10.1016/j.cej.2011.09.091
74. Castro G.A.D., Batista R.C., De Sousa R. de C.S., Carneiro A. de C.O., Fernandes S.A. Green synthesis of furfural from xylose and corn cob biomas. *React. Chem. Eng.* 2023;(8):1969–1980. https://doi.org/10.1039/D3RE00017F
75. Chen Z., Reznicek W.D., Wan C. Aqueous choline chloride: A novel solvent for switchgrass fractionation and subsequent hemicellulose conversion into furfural. *ACS Sustain. Chem. Eng.* 2018;6(8):6910–6919. https://doi.org/10.1021/acssuschemeng.8b00728
76. Lee C.B.T.L., Wu T.Y., Cheng C.K., Siow L.F., Chew I.M.L. Nonsevere furfural production using ultrasonicated oil palm fronds and aqueous choline chloride-oxalic acid. *Ind. Crops Prod.* 2021;166:113397. https://doi.org/10.1016/j.indcrop.2021.113397
77. Eifert T., Liauw M.A. Process analytical technology (PAT) applied to biomass valorisation: a kinetic study on the multiphase dehydration of xylose to furfural. *React. Chem. Eng.* 2016;1(5):521–532. https://doi.org/10.1039/C6RE00082G
78. Scapin E., Rambo M.K.D., Viana G.C.C., *et al.* Sustainable production of furfural and 5-hidroximetilfurfural from rice husks and soybean peel by using ionic liquid. *Food Sci. Technol.* 2020;40(Suppl. 1):83–87. https://doi.org/10.1590/fst.04419
79. Lin K.-H., Huang M.-H., Chang A.C.-C. Liquid phase reforming of rice straw for furfural production. *Int. J. Hydrogen Energy*. 2013;38(35):15794–15800. https://doi.org/10.1016/j.ijhydene.2013.06.088
80. Dussan K., Girisuta B., Haverty D., Leahy J.J., Hayes M.H.B. Kinetics of levulinic acid and furfural production from *Miscanthus x giganteus*. *Bioresour. Technol.* 2013;149:216–224. https://doi.org/10.1016/j.biortech.2013.09.006
81. Al Rashdi S., Al Balushi A., Patil G. Optimized extraction of furfural from omani date palm seeds: A comparative study of soxhlet and distillation techniques. *Multidiscip. Sci. J.* 2025;7:e2025005. https://doi.org/10.31893/multiscience.2025005
82. Al-Rahbi B.S.N., Dwivedi P.B. Extraction and characterization of furfural from waste Omani date seeds. *Green Chem. Technol. Lett.* 2016;2(4):219–223. https://doi.org/10.18510/gctl.2016.249
83. Sweygers N., Depuydt D.E.C., Vuure A.W.V., *et al.* Simultaneous production of 5-hydroxymethylfurfural and furfural from bamboo (*Phyllostachys nigra* 'Boryana') in a biphasic reaction system. *Chem. Eng. J.* 2020;386:123957. https://doi.org/10.1016/j.cej.2019.123957
84. Xia Q., Peng H., Zhang Y., *et al.* Microwave-assisted furfural production from xylose and bamboo hemicellulose in a biphasic medium. *Biomass Convers. Bioref.* 2021;13(9):7895–7907. https://doi.org/10.1007/s13399-021-01870-7
85. Senila L., Miclean M., Senila M., Roman M., Roman C. New analysis method of furfural obtained from wood applying an autohydrolysis pretreatment. *Rom. Biotechnol. Lett.* 2013;18(1):7947–7955. Available: https://www.biotehgen.eu/RBL/8 Senila.pdf. Accessed January 5, 2025.
86. Gao H., Liu H., Pang B., *et al.* Production of furfural from waste aqueous hemicellulose solution of hardwood over ZSM-5 zeolite. *Bioresour. Technol.* 2014;172:453–456. https://doi.org/10.1016/j.biortech.2014.09.026
87. Liu H., Hu H., Jahan M.S., Ni Y. Furfural formation from the pre-hydrolysis liquor of a hardwood kraft-based dissolving pulp production process. *Bioresour. Technol.* 2013;131:315–320. https://doi.org/10.1016/j.biortech.2012.12.158
88. Ntimbani R.N., Farzad S., Görgens J.F. Furfural production from sugarcane bagasse along with co-production of ethanol from furfural residues. *Biomass Convers. Bioref.* 2021;12:5257–5267. https://doi.org/10.1007/s13399-021-01313-3
89. Rivera-Cedillo E.E., González-Chávez M.M., Handy B.E., Quintana-Olivera M.F., López-Mercado J., Cárdenas-Galindo M. Acid-catalyzed transformation of orange waste into furfural: the effect of pectin degree of esterification. *Bioresour. Bioprocess.* 2024;11:52. https://doi.org/10.1186/s40643-024-00768-2
90. Sattar M.A., Chakraborty A.K., Al-Reza S.M., Islam S. Extraction and estimation of furfural from decorative plants grown in Bangladesh. *Bangladesh J. Sci. Ind. Res.* 2007;42(4):495–498. https://doi.org/10.3329/bjsir.v42i4.759
91. Iriany I., Taslim T., Bani O., Pratama A.J. Potential of lime as a green catalyst in the manufacture of furfural from *Mikania micrantha*. *IOP Conf. Ser.: Earth Environ.* 2021;713(1):012038. http://doi.org/10.1088/1755-1315/713/1/012038

92. Uy J.R., Careo N.D., Llarena D., Barajas J.R. Optimization of furfural extraction from *Theobrama* cacao wastes using response surface methodology. *MATEC Web Conf.* (*RSCE 2018*). 2019;268(4):06010. https://doi.org/10.1051/MATECCONF/201926806010
93. Huang L., Peng H., Xiao Z., *et al.* Production of furfural and 5-hydroxymethyl furfural from *Camellia oleifera* fruit shell in [Bmim]HSO_4/H_2O/1,4-dioxane biphasic medium. *Ind. Crops Prod.* 2022;184(18):15006. https://doi.org/10.1016/j.indcrop.2022.115006
94. Liu L., Chang H.-M., Jameel H., Park S. Furfural production from biomass pretreatment hydrolysate using vapor-releasing reactor system. *Bioresour. Technol.* 2018;252: 165–171. https://doi.org/10.1016/j.biortech.2018.01.006
95. Stamigna C., Chiaretti D., Chiaretti E., Prosini P.P. Oil and furfural recovery from *Brassica carinata. Biomass and Bioenergy*. 2012;39:478–483. https://doi.org/10.1016/j.biombioe.2011.12.024
96. Gong L., Zha J., Pan L., Ma C., He Y.-C. Highly efficient conversion of sunflower stalk-hydrolysate to furfural by sunflower stalk residue-derived carbonaceous solid acid in deep eutectic solvent/organic solvent system. *Bioresour. Technol.* 2022;351:126945. https://doi.org/10.1016/j.biortech.2022.126945
97. Zha J., Fan B., He J., He Y.-C., Ma C. Valorization of biomass to furfural by chestnut shell-based solid acid in methyl isobutyl ketone–water–sodium chloride system. *Appl. Biochem. Biotechnol.* 2022;194:2021–2035. https://doi.org/10.1007/s12010-021-03733-3
98. Yue Z., Sun L.-L., Wen J.-L., Yao S.-Q., Sun S.-N., Cao X.-F. Simultaneous production of furfural, lignin and cellulose-rich residue from by ChCl/1,2-propanediol/MIBK biphasic system pretreatment. *Int. J. Biol. Macromol.* 2024;271(Part 1):133522. https://doi.org/10.1016/j.ijbiomac.2024.133522
99. Adebayo A.J., Ogunjobi J.K., Oluwasina O.O., Lajide L. Comparative production and optimisation of furfural and furfuryl alcohol from agricultural wastes. *Chem. Africa*. 2023;6:2401–2417. https://doi.org/10.1007/s42250-023-00594-7
100. Dutta S., De S., Saha B., Alam I. Advances in conversion of hemicellulosic biomass to furfural and upgrading to biofuels. *Catal. Sci. Technol.* 2012;2(10):2025–2036. https://doi.org/10.1039/c2cy20235b
101. Cai C.M., Zhang T., Kumar R., Wyman C.E. Integrated furfural production as a renewable fuel and chemical platform from lignocellulosic biomass. *J. Chem. Technol. Biotechnol.* 2014;89(1):2–10. https://doi.org/10.1002/jctb.4168
102. Piñeiro-García A., González-Alatorre G., Vega-Díaz S.M., Pérez-Pérez M.C.I., Tristan F., Patiño-Herrera R. Reduced graphene oxide coating with high performance for the solid phase micro-extraction of furfural in espresso coffee. *J. Food Meas. Charact.* 2019;14(4):314–321. https://doi.org/10.1007/s11694-019-00293-3
103. Jung K., You S.K., Moon S., Lee U. Furfural from pine needle extract inhibits the growth of a plant pathogenic fungus, *Alternaria mali*. *Mycobiology*. 2018;35(1):39–43. https://doi.org/10.4489/MYCO.2007.35.1.039
104. Zhuang Y., Si Z., Pang S., Wu H., Zhang X., Qin P. Recent progress in pervaporation membranes for furfural recovery: A mini review. *J. Clean. Prod.* 2023;396:136481. https://doi.org/10.1016/j.jclepro.2023.136481
105. Ambalkar V.U., Talib M.I. Synthesis of furfural from lignocellulosic biomass as agricultural residues: A review. *Int. J. Eng. Sci.* 2012;1(1):30–36. Available: http://www.theijes.com/papers/v1-i1/G011030036.pdf. Accessed January 5, 2025.
106. Hidajati N. The treatment of the corn-knob as a raw material for making furfural. *J. Ilmu Dasar*. 2007;8(1):45–53. Available: https://jurnal.unej.ac.id/index.php/JID/article/view/129. Accessed January 5, 2025.
107. Nsubuga H., Basheer C., Al-Muallem H.A.S., Kalanthoden A.N. Isolation, characterization and evaluation of photochemical potential of rice husk-based furfural via continuous fl ow reactor. *J. Environ. Chem. Eng.* 2016;4(1): 857–863. https://doi.org/10.1016/j.jece.2015.12.026
108. Li Q., Ma C.-L., Zhang P.-Q., Li Y.-Y., Zhu X., He Y.-C. Effective conversion of sugarcane bagasse to furfural by coconut shell activated carbon-based solid acid for enhancing whole-cell biosynthesis of furfurylamine. *Ind. Crop. Prod.* 2020;160:113169. https://doi.org/10.1016/j.indcrop.2020.113169
109. Sherif N., Gadalla M., Kamel D. Acid–hydrolysed furfural production from rice straw bio-waste: Process synthesis, simulation, and optimisation. *South African J. Chem. Eng.* 2021;38:34–40. https://doi.org/10.1016/j.sajce.2021.08.002
110. Contreras-Zarazúa G., Martin-Martin M., Sanchez-Ramirez E., Segovia-Hernandez J.G. Furfural production from agricultural residues using different intensified separation and pretreatment alternatives . Economic and environmental assessment. *Chem. Eng. Process. Intensif.* 2021;171:108569. https://doi.org/10.1016/j.cep.2021.108569
111. Li X., Liu Q., Luo C., Gu X., Lu L., Lu X. Kinetics of furfural production from corn cob in γ-Valerolactone using dilute sulfuric acid as catalyst. *ACS Sustain. Chem. Eng.* 2017;5(10): 8587–8593. https://doi.org/10.1021/acssuschemeng.7b00950
112. Xiang Z., Runge T. Co-production of feed and furfural from dried distillers' grains to improve corn ethanol profitability. *Ind. Crop. Prod.* 2014;55:207–216. https://doi.org/10.1016/j.indcrop.2014.02.025
113. Ye L., Han Y., Wang X., Lu X., Qi X., Yu H. Recent progress in furfural production from hemicellulose and its derivatives: Conversion mechanism, catalytic system, solvent selection. *Mol. Catal.* 2021;515:111899. https://doi.org/10.1016/j.mcat.2021.111899
114. Cousin E., Namhaed K., Pérès Y., *et al.* Towards efficient and greener processes for furfural production from biomass: A review of the recent trends. *Sci. Total Environ.* 2022;847: 157599. https://doi.org/10.1016/j.scitotenv.2022.157599
115. Iroha N.B., Akaranta O., James A.O. Red onion skin extract-furfural resin as corrosion inhibitor for aluminium in acid medium. *Der Chem. Sin.* 2012;3(4):995–1001. Available: http://www.pelagiaresearchlibrary.com/der-chemica-sinica/vol3-iss4/DCS-2012-3-4-995-1001.pdf. Accessed January 5, 2025.
116. Nie Y., Hou Q., Li W., Bai C., Bai X., Ju M. Efficient synthesis of furfural from biomass using $SnCl_4$ as catalyst in ionic liquid. *Molecules*. 2019;24(3):594. https://doi.org/10.3390/molecules24030594
117. LaForge F.B. The production of furfural by the action of superheated water on aqueous corncob extract. *J. Ind. Eng. Chem.* 2000;13(11):1024–1025. https://doi.org/10.1021/ie50143a029
118. Li H., Dai Q., Ren J., *et al.* Effect of structural characteristics of corncob hemicelluloses fractionated by graded ethanol precipitation on furfural production. *Carbohydr. Polym.* 2016;136:203–209. https://doi.org/10.1016/j.carbpol.2015.09.045
119. Edumujeze D., Fournier-Salaün M.-C., Leveneur S. Production of furfural: From kinetics to process assessment. *Fuel*. 2025;381(Part B):133423. https://doi.org/10.1016/j.fuel.2024.133423

120. Mazar A., Jemaa N., Al Dajani W.W., Marinova M., Perrier M. Furfural production from a pre-hydrolysate generated using aspen and maple chips. *Biomass and Bioenergy*. 2017;104: 8–16. https://doi.org/10.1016/j.biombioe.2017.05.016
121. Noda T., Takahata Y., Sato T. Sugar composition of cell wall material from sweet potatoes differing in stages of development, tissue zone and variety. *Oyo Toshitsu Kagaku*. 1994;41(3):311–316. Available: https://www.jstage.jst.go.jp/article/jag1994/41/3/41_3_311/_pdf. Accessed January 5, 2025.
122. Dias A.S., Lima S., Pillinger M., Valente A.A. Furfural and furfural-based industrial chemicals. In: Pignataro B. (Ed.). *Ideas in Chemistry and Molecular Sciences: Advances in Synthetic Chemistry. Part III. Chemical Reactions, Sustainable Processes, and Environment.* Weinheim: WILEY-VCH Verlag GmbH & Co. KGaA; 2010. Ch. 8. P. 165–185. https://doi.org/10.1002/9783527630554.ch8
123. Xu W., Zhang S., Lu J., Cai Q. Furfural production from corncobs using Thiourea as additive. *Environ. Prog. Sustain. Energy*. 2017;36(3):690–695. https://doi.org/10.1002/ep.12489
124. Jorqueira D.S.S., de Lima L.F., Maya S.F., *et al.* Critical review of furfural and furfuryl alcohol production: Past, present, and future on heterogeneous catalysis. *Appl. Catal. A: Gen.* 2023;665:119360. https://doi.org/10.1016/j.apcata.2023.119360

About the Authors

Abdulhalim Musa Abubakar, Master (Eng.), Lecturer, Department of Chemical Engineering, Faculty of Engineering, Modibbo Adama University, P.M.B. 2076, Yola, Adamawa State, Nigeria). E-mail: abdulhalim@mau.edu.ng. Scopus Author ID 58150539400, https://orcid.org/0000-0002-1304-3515

Iyisikwe Tanimu Umar, Bachelor (Eng.), Undergraduate Student, Department of Chemical Engineering, Faculty of Engineering, Modibbo Adama Federal University of Technology (P.M.B. 2076, Yola, Adamawa State, Nigeria). E-mail: iyisikwetanimu@gmail.com.

Abass-Giwa Muhammed Akintunde, Bachelor (Eng.), Undergraduate Student, Department of Chemical Engineering, Faculty of Engineering, University of Maiduguri (P.M.B. 1069, Bama Road, Maiduguri, Borno State, Nigeria). E-mail: akintundemuhammedabass-giwa@unimaid.edu.ng. https://orcid.org/0009-0003-3047-3116

Muhammad Jimada Aliyu, Bachelor (Eng.), Graduate Trainee Engineer, Chemical Engineering Department, School of Infrastructure, Process Engineering and Technology, Federal University of Technology (P.M.B. 65, Minna, Niger State, Nigeria). E-mail: ajimada.m1600354@st.futminna.edu.ng. https://orcid.org/0009-0006-0592-8985

Marwea Al-Hedrewy, PhD., Associate Professor, College of Technical Engineering, the Islamic University, Najaf, Iraq; College of Technical Engineering, the Islamic University of Al Diwaniyah, Al Diwaniyah, Iraq. E-mail: mereng@iunajaf.edu.iq. Scopus Author ID 59331742300, https://orcid.org/0009-0008-7371-6364

Uday Raheja, Bachelor (Eng.), Student, Center for Research Impact & Outcome, Chitkara University Institute of Engineering and Technology (CUIET), Chitkara University (140401, Rajpura, Punjab, India). E-mail: uday_raheja@outlook.com. https://orcid.org/0009-0000-6546-279X

The text was submitted by the authors in English
and edited for English language and spelling by Thomas A. Beavitt